Development of integrated demand and supply side management strategy of multi-energy system for residential building application

X.J. Luo, K.F. Fong*

Division of Building Science and Technology, College of Science and Engineering, City University of Hong Kong

*Corresponding author

Email address: bssquare@cityu.edu.hk

Postal address: Tat Chee Avenue, Kowloon, Hong Kong, China

Abstract

The multi-energy system (MES) that contains the highly coupled energy supply equipment units can be adopted to simultaneously satisfy the cooling, heating and electrical energy demands. Owing to the complex nature of multiple supplies and demands, an integrated demand and supply side management (IDSSM) strategy was proposed for aligning the MES operation and the building demands. The IDSSM strategy included three core algorithms: Demand side rolling optimization (DSRO), supply side rolling optimization (SSRO) and feedback correction (FC). DSRO was implemented to decide the schedulable appliances over the next 24-h planning horizon, while SSRO was adopted to determine the operating capacities of energy supply equipment units. FC was involved for continual modification on any discrepancy between various actual and predicted energy demands. In this study, a trigeneration system primed with solid oxide fuel cell-gas turbine (SOFC-GT) was designed as the MES to serve a high-rise apartment building with electric cars. It was found that the primary energy consumption, the design capacity of the SOFC-GT set and the capacity of electricity storage would be decreased by 8.75%, 10% and 43% respectively when SSRO integrated with DSRO. It was also noted that electric cars played an important role in effective demand side management.

Keywords: Multi-energy system; Demand side management; Supply side management; Rolling optimization; Feedback correction; Electric car.

1. Introduction

Accounting for above one-third of primary energy consumption globally, buildings have become the largest energy-consuming sector [1]. For sustainable urbanization, integrated approach of various energy supplies is getting popular in building design, causing the rise of multi-energy system (MES) [2,3]. It is common to design MES able to simultaneously satisfy different demands in buildings, like cooling, heating and electricity. Meanwhile, various energy storages, such as cool, heat and electricity storages can be equipped for load shifting purposes. On the one hand, the MES involves multiple energy supply equipment units with highly coupled nature; on the other hand, various and changing energy demands were required by the building. Therefore, it is necessary to develop an effective control scheme to properly coordinate the supply and demand side management of various energy types.

In previous research, most of the control strategies for MES were developed using optimization algorithms including evolutionary algorithms [4, 5] as well as mixed-integer linear programming [6-9]. In these control strategies, objective function was defined from energy, environmental and economy point of view. The optimization algorithms were thus adopted to regulate the control variables of critical equipment units, such as prime mover, absorption chiller, compression chiller, auxiliary boiler and energy storages. The optimization constraints mainly included energy balances and equipment operating constraints. However, these control strategies focused only on the supply side management (SSM) of MES.

Generally, there existed peak energy demands during certain periods, such as peak cooling demand of office buildings in the afternoon and peak electricity demand of residential buildings at night. At the supply side, energy storages could be installed to shift the peak energy production. In other words, they could be charged to store energy when there was surplus production, and discharged to supplement the peak demand. Therefore, the actual peak energy production would be lower than the corresponding demand. However, there would be energy loss during the charging and discharging processes. Moreover, energy storages would cause additional capital cost and spatial requirements. If part of the peak energy demands could be shifted through appropriate demand side management (DSM), the overall energy consumption and investment cost may be reduced.

DSM means shifting the peak energy demands through rescheduling the operating durations of electrical appliances at the demand side. Previously, DSM was mainly conducted through incentive-based and price-based optimizations. In incentive-based optimization, a reward was guaranteed to customers for providing energy consumption reduction when there was a peak demand. Price-based optimization, namely dynamic pricing scheduling, meant encouraging customers to change the

operating period of certain electrical appliances according to the dynamic electricity price. For incentive-based DSM methods, predicted energy demands were needed before determining the incentive and price schemes.

There were some previous works regarding incorporating incentive-based or price-based DSM into SSM to improve system performance. The dispatching schedules of energy supply equipment units and operating durations of electrical appliances were determined based on minimizing total operating cost. Different optimization algorithms, such as genetic algorithm [10], mixed integer nonlinear programming [11-17] and liner programing [18] were generally used to solve the objective functions. From these studies, it is seen that by integrating DSM with SSM, the peak energy demands could be shifted and thus resulted in more appropriate operating schedules of the energy supply equipment units. However, in most of these studies [10-18], only the electrical energy was considered, and the city power grid was used as the primary electricity supplier. Although the MES was mentioned in [19-22], the predicted dynamic price schemes were required to implement the price-based and incentive-based DSM methods. Thus the effectiveness of the energy management was affected by the availability and accuracy of such predicted dynamic incentive or price schemes. Moreover, the complicated interactions among different energy supplies were not considered in these studies. In addition, thermodynamic models of equipment units in above-mentioned studies were usually simplified: They were assumed to operate at steady-state with constant efficiency. As a result, dynamic responses of the equipment units were overlooked for performance assessment of those proposed energy management methods. Besides, the role of electric vehicles in DSM and energy storage is getting paramount. In [23-26], the scheduling strategy of electric vehicles was proposed in the microgrid. Due to the merit of tariff structure, it was found that the electric cars were charged during the hours with lower electricity prices while discharged during the periods with higher electricity prices to sell the stored energy. In building applications, the potential contribution of electric cars associated to MES is seldom explored.

Therefore, the objective of this research work was to propose an integrated demand and supply side management (IDSSM) method, which was expected to be effective for daily operation of both the MES and electrical appliances for an apartment building under changing weather conditions. Firstly, schedulable electrical appliances in the apartment building were identified. Meanwhile, the complicated and dynamic system model of the MES was built to have a better understanding of the system performances under various operating conditions. For the MES, a trigeneration primed with solid oxide fuel cell-gas turbine (SOFC-GT) set was used so as to fully utilize its high electrical efficiency while city power grid was connected for standby purpose. The SOFC-GT trigeneration system, accompanied with cooling, heating and electricity storages, was regarded as the MES in this study.

2. Development of reference apartment building

To investigate the capability of the proposed IDSSM method, a reference high-rise apartment was used. It has 30 floors and the floor layout is shown in Fig. 1. There were two types of sample flat: 4-bedroom flat and 3-bedroom flat. On each floor, there were 2 former flats and 4 latter ones. The floor, wall and window areas of each type of sample flat are summarized in Tables 1 and 2, which were set with reference to [27-30].

Fig. 1. Typical floor layout plan and sample flats of reference apartment building.

Table 1. Floor area of the sample flats.

	Floor area (m^2)	
	4-bedroom flat	3-bedroom flat
Bedroom 1	10.0	12.8
Bedroom 2	5.0	4.7
Bedroom 3	10.0	4.7
Bedroom 4	5.0	NA
Living room	37.5	34.4
Kitchen	9.7	5.3
Bathroom 1	4.3	3.7
Bathroom 2	4.3	3.7
Total	85.8	69.3

Table 2. Area of wall and window of the sample flats.

	Area (m^2)			
	4-bedroom flat		3-bedroom flat	
	Wall	Windows	Wall	Windows
North	20.76	5.02	45.97	5.34
West	27.04	7.94	10.74	0
South	20.76	0	45.97	12.31
East	27.04	7.94	10.74	6.20
Total	95.60	20.9	113.42	17.65

For the apartment building, it was assumed that centralized cooling and heating supplies were provided. The indoor design information was applied according to the local engineering practice [31,32] and listed in Table 3. The daily occupancy and lighting schedules are presented in Figs. 2 and 3, respectively, which were set according to [27-30].

Table 3. Indoor design criteria of the apartment building.

Item		Design criterion
Indoor design temperature	Summer	24 °C
	Winter	20 °C
Indoor design relative humidity		55%
Outdoor fresh air requirement		8 L/s/person
Hot water requirement	For bath	15 L/person/day
	For drinking	0.2 L/person/h
Temperature set-point of hot water	For bath	80 °C
Lighting power intensity	Bedroom	16.33 W/m^2
	Living room	19.73 W/m^2
	Kitchen	15.81 W/m^2
	Bathroom	20.67 W/m^2
Equipment power intensity	Bedroom	23.53 W/m^2
	Living room	27.22 W/m^2
	Kitchen	518.64 W/m^2
	For drinking	100 °C
Quantity of lift		2
Lift power requirement		2 kW/lift

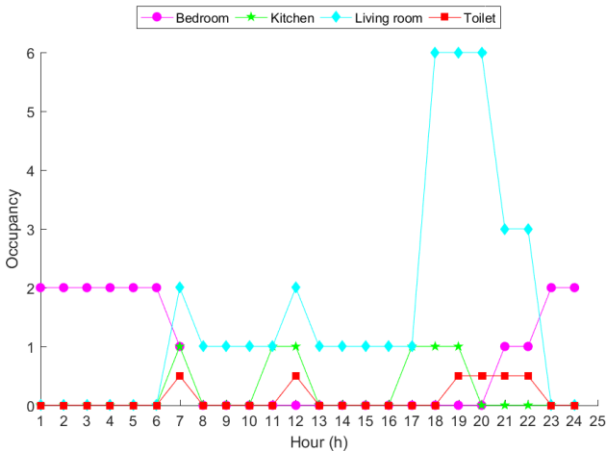

Fig. 2. Daily occupancy schedule.

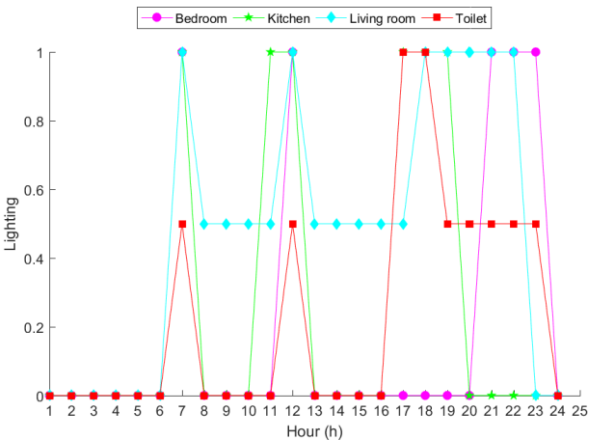

Fig. 3. Daily lighting schedule.

To assess the various building energy demands in four seasons, typical days in each season were chosen to represent the respective seasons. To determine the predicted cooling demand $D_{c,p}$ and the predicted heating demand $D_{h,p}$, those values from the typical meteorological year of Hong Kong [33] were adopted as the forecasting values of ambient air dry-bulb temperature $T_{db,f}$ and relative humidity RH_f. In practical application, such information can be acquired from the weather forecast website [34]. On the other hand, the actual cooling demand was determined by the real-time ambient air dry-bulb temperature $T_{db,r}$ and the real-time relative humidity RH_r, which were acquired from those hour-ahead forecasting values. In this study, the deviations between the real-time weather data and those corresponding forecast values were assumed to follow normal distributions, with an error range within ± 0.5 °C for temperature and ± 5% for relative humidity [35].

Based on these forecasting values of weather data in Fig. 4 as well as operating schedules of occupancy and lighting in Figs. 2 and 3, $D_{c,p}$ and $D_{h,p}$ could be obtained, as shown in Figs. 5 and 6. Meanwhile, the real-time weather data is also shown in Fig. 4. Based on these assumed real-time values, the actual real-time cooling demand $D_{c,r}$ and the real-time heating demand $D_{h,r}$ were obtained, as shown in Figs. 5 and 6 respectively. In this study, since Hong Kong has of sub-tropical climate, space heating was only needed in winter. In other seasons, heating demand was only needed for heating up drinking and bathing water.

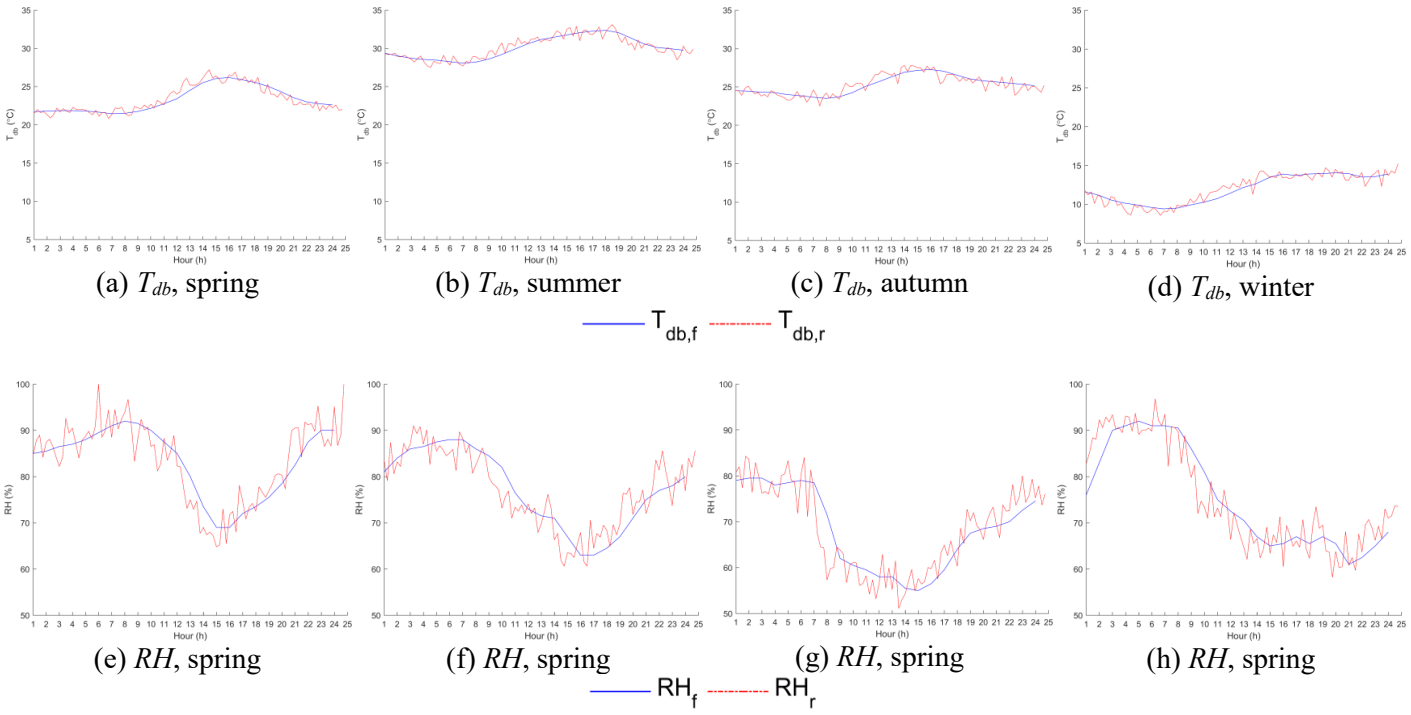

(a) T_{db}, spring (b) T_{db}, summer (c) T_{db}, autumn (d) T_{db}, winter

(e) RH, spring (f) RH, spring (g) RH, spring (h) RH, spring

Fig. 4. Forecasted and real-time weather data.

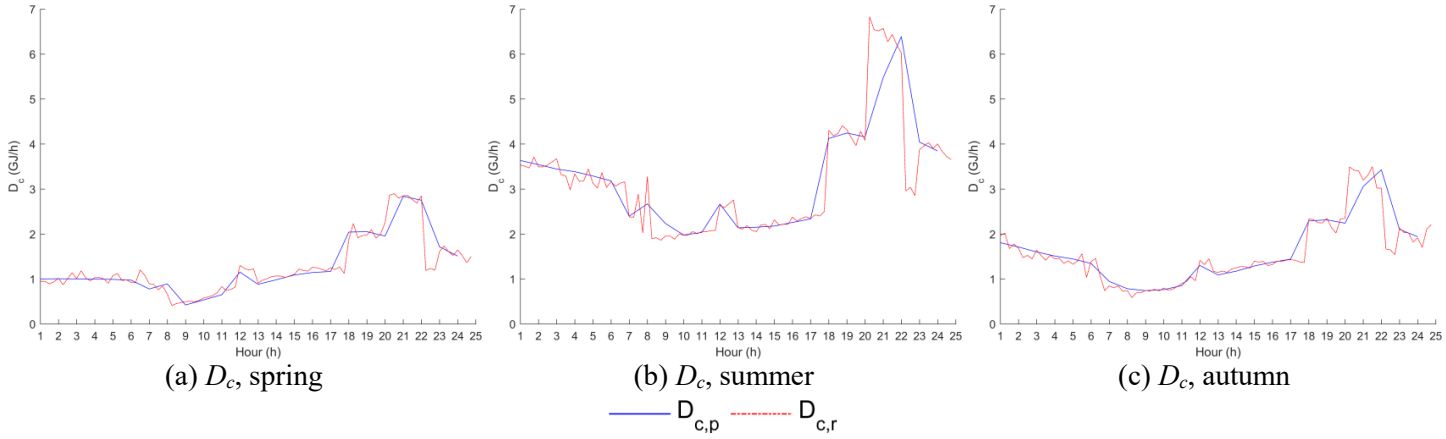

(a) D_c, spring (b) D_c, summer (c) D_c, autumn

Fig. 5. Predicted and real-time cooling energy demand in four seasons.

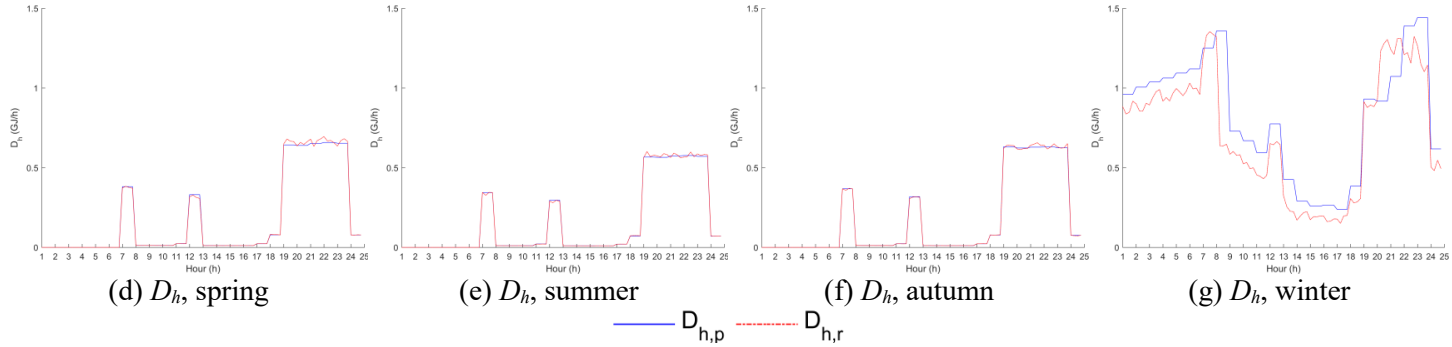

(d) D_h, spring (e) D_h, summer (f) D_h, autumn (g) D_h, winter

Fig. 6. Predicted and real-time heating energy demand in four seasons.

The basic electricity demand $D_{e,b}$ of the high-rise apartment building consisted of power consumption of non-schedulable electrical appliances P_{ns} and schedulable electrical appliances P_{sch}. The operating schedules of these electrical appliances are summarized in Table 4. The non-schedulable electricity demands referred to the power consumption of lighting, lifts and non-schedulable electrical appliances including cooking equipment, desktop computers, refrigerators and TV. On the other hand, schedulable electrical energy demands included those from dish washers, washing machine, vacuum cleaner and electric cars.

Table 4. Operating schedules of residential electrical appliances.

Type	Electrical appliances	Originally scheduled operating duration	Total operating duration d (h)	Power consumption (kW)	Quantity per flat	Allowed schedulable operating duration
Non-schedulable electrical appliances	Cooking equipment	7^{th}, 12^{th} and 18^{th} h	3	1.3	1	NA
	Desktop computer	18^{th} - 22^{nd} h	5	0.2	3 for 3-bedroom flat; 4 for 4-bedroom flat	NA
	Refrigerator	1^{st} - 24^{th} h	24	0.0417	1	NA
	TV	18^{th} - 23^{rd} h	6	0.15	2 for 3-bedroom flat; 3 for 4-bedroom flat	NA
Schedulable electrical appliances	Washing machine	19^{th} h	3	1	1	7^{th} - 21^{st} h
	Dish washer	8^{th}, 13^{th}, 19^{th} h	1	1.5	1	8^{th} - 11^{th} h, 13^{th} - 17^{th} h, 19^{th} - 22^{nd} h
	Vacuum cleaner	19^{th} h	1	0.6	1	7^{th} - 21^{st} h
	Electric cars	18^{th} - 20^{th} h	3	3.5	2	19^{th}- 24^{th} h and 1^{st} - 7^{th} h

3. Development of MES dynamic model

A complex MES was used to simultaneously satisfy the cooling, heating and electricity demands of the high-rise apartment building. In this study, a SOFC-GT primed trigeneration system with cool storage, heat storage and electricity storage was developed to evaluate the proposed IDSSM strategy.

3.1 System design

The schematic design of the MES is shown in Fig. 7. The SOFC-GT set was used as the main electricity generation unit, while city power grid was only connected for emergency purpose. Apart from satisfying the basic electricity demand D_e of the apartment building, the electricity generated by the SOFC-GT set was also used to supply electricity for the compression chillers P_{CoC} and the parasitic components P_{para} including various water pumps, cooling towers and air handling units. Thus, the overall electricity demand $D_{e,t}$ was the total of D_e, P_{CoC} and P_{para}.

After exiting the SOFC-GT set, the hot exhaust gas was recovered through the heat recovery system, which was used to supply thermal energy for space heating, drinking and bathing water heating, as well as hot water for absorption chiller through various heat exchangers. Meanwhile, both absorption chiller (AbC) and compression chillers (CoC) were used to satisfy cooling demand of the high-rise apartment building. To facilitate better supply side energy management, the design of this MES was featured with the cool storage (CS), heat storage (HS) and electricity storage (ES) for diverse load

shifting purposes. When necessary, the corresponding energy storage would be discharged or charged to coordinate the operation of other energy supply equipment units.

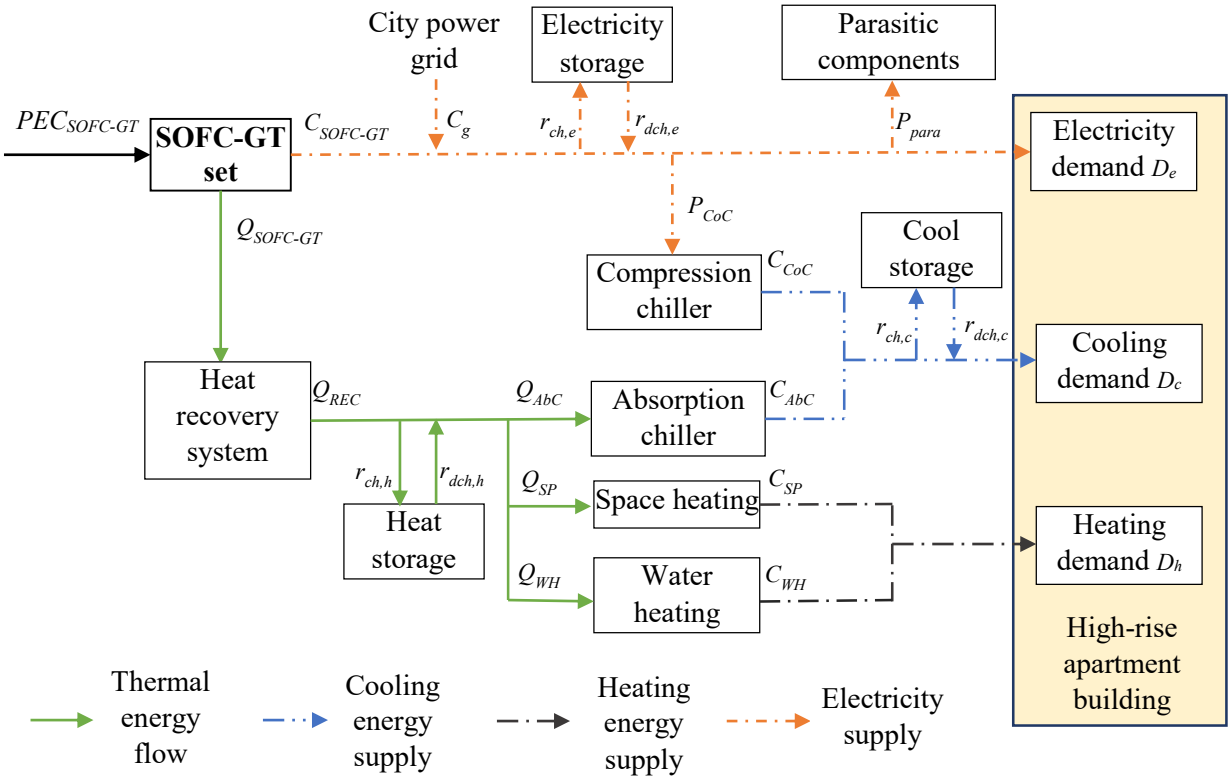

Fig. 7. Schematic design of MES.

To consider the effects of ambient air and loading conditions on the entire MES, the dynamic models of SOFC-GT set, AbC and CoC from our previous studies [36-38] were used. Thus, the changing efficiency at part-load operation could be accounted. The performance curves of the SOFC-GT set, AbC and CoC are shown in Fig. 8.

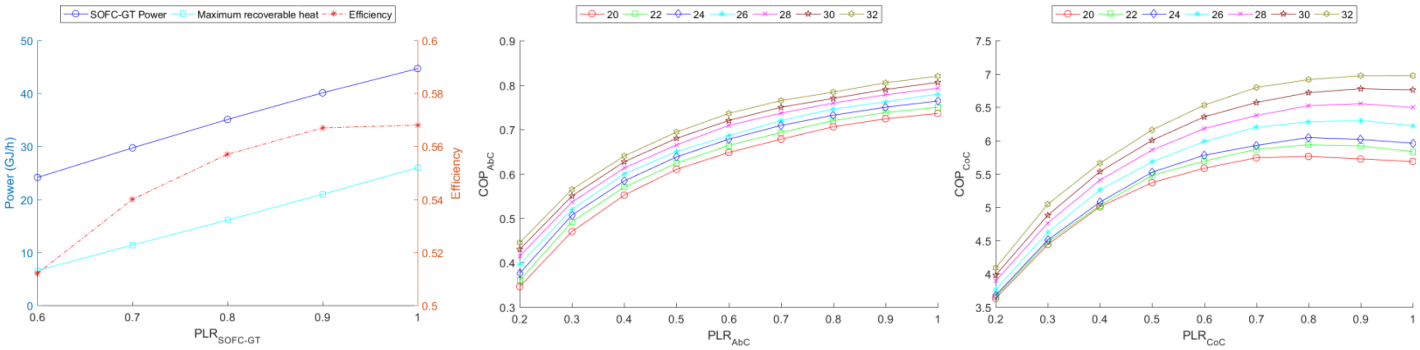

(a) SOFC-GT set. (b) AbC (c) CoC

Fig. 8. Performance curves of the major equipment units of MES.

The electrical efficiency and power output of the SOFC-GT set at different part load ratios (*PLR*s) could be obtained from Fig. 8(a), while the coefficient of performance (COP) of both AbC and CoC at different *PLR*s could be got from the corresponding performance curves in Figs. 8(b) and 8(c) respectively.

3.2 Determining the design parameters for equipment units

The design capacities of each equipment unit were determined on the condition that DSM was not implemented, since they may be larger when SSM was not integrated with DSM. Various energy storages (i.e. CS, HS and ES) were able to shift the peak energy demands thus facilitate the effective operation of the MES. The principle in capacity allocation among energy storages and related equipment units were similar to that adopted in our previous research [36]. The design capacities of each equipment unit is summarized in Table 5, accompanied by the other key system design information. On the basis of the profile of cooling among different seasons, five identical CoCs were adopted. And there would be two, five and three CoCs operating in spring, summer and autumn, respectively.

Table 5. Design parameters of major equipment units in MES.

Design parameter	**Value**
Design capacity of SOFC-GT set ($GJ \cdot h^{-1}$)	4.5
$PLR_{SOFC\text{-}GT}$ range	[0.6, 1]
Design capacity of AbC ($GJ \cdot h^{-1}$)	1.2
Design capacity of CoC ($GJ \cdot h^{-1}$)	0.6
Design capacity of CS (GJ)	14
Design capacity of HS (GJ)	9
Design capacity of ES (GJ)	40
Efficiency of heat exchangers (%)	80
Potable water pumps efficiency (%)	60
Set-point of chilled water supply temperature (°C)	7
Efficiency of chilled water pump (%)	60
Efficiency of cooling water pump (%)	60
Efficiency of hot water pump (%)	60
Cooling tower fan efficiency (%)	80
Design flow rate of hot water in each AbC ($kg \cdot h^{-1}$)	95465
Design flow rate of chilled water in each AbC ($kg \cdot h^{-1}$)	57279
Design flow rate of cooling water in each AbC ($kg \cdot h^{-1}$)	28640
Design flow rate of chilled water in each CoC ($kg \cdot h^{-1}$)	143200
Design flow rate of cooling water in each CoC ($kg \cdot h^{-1}$)	71599
CS charging efficiency (%)	90
CS discharging efficiency (%)	90
HS charging efficiency (%)	90
HS discharging efficiency (%)	90
ES charging efficiency (%)	95
ES discharging efficiency (%)	85
Efficiency of CS water pump (%)	60
Efficiency of HS water pump (%)	60
Efficiency of supply air fan (%)	65
Efficiency of supply air cooling coil (%)	70
Efficiency of supply air heating coil (%)	70

4. Formulation of the IDSSM strategy

At the demand side, electric cars and various electrical appliances could be scheduled to reduce the peak value of basic electricity demand D_e. At the supply side, different types of energy were generated from the MES to satisfy corresponding demands of the high-rise apartment building. To better coordinate the multiple energy demands and supplies, the IDSSM strategy was formulated by integrating DSM with SSM. The proposed strategy aimed at effectively coordinating the schedulable electrical demands in the building and the highly coupled energy supply equipment units in MES. The IDSSM strategy consists of three core algorithms, demand side rolling optimization (DSRO), supply side rolling optimization (SSRO) and feedback correction (FC). The flow of the entire IDSSM strategy is illustrated in Fig. 9, which will be discussed in the following sub-sections.

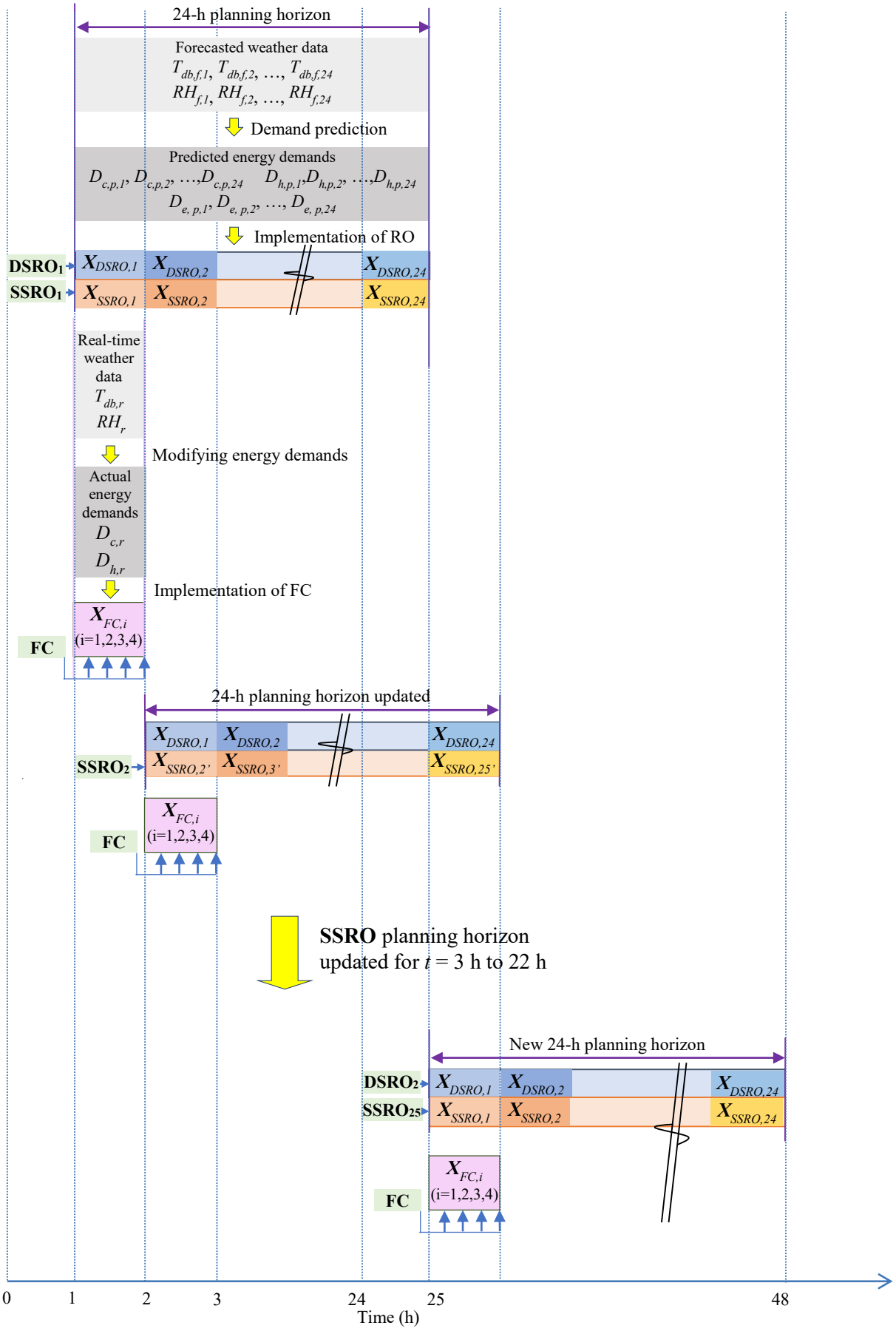

Fig. 9. The flow of IDSSM strategy.

4.1 DSRO and SSRO algorithms

Both DSRO and SSRO algorithms were constructed using the approach of model predictive control. As shown in Fig. 9, at t = 0 h on each day, on the basis of predicted cooling, heating and basic electricity demands (i.e. $D_{c,p}$, $D_{h,p}$ and $D_{e,p}$) during 1-24 h, DSRO and SSRO were simultaneously implemented. The aim of DSRO was to determine the operating schedule $\mathbf{X_{DSRO}}$ = ($\boldsymbol{X}_{DSRO,1}$, $\boldsymbol{X}_{DSRO,2}$, …, $\boldsymbol{X}_{DSRO,24}$) of the schedulable electrical appliances, which included washing machines, dish washers, vacuum cleaners and electric cars as illustrated in Table 4 before. The objective of SSRO was to determine the optimal control variables $\mathbf{X_{SSRO}}$ = ($\boldsymbol{X}_{SSRO,1}$, $\boldsymbol{X}_{SSRO,2}$, …, $\boldsymbol{X}_{SSRO,24}$) of the related supply equipment units in the MES. To take the entire daily energy demand profiles into account, $\mathbf{X_{DSRO}}$ and $\mathbf{X_{SSRO}}$ were determined to minimize of the primary energy consumption over a 24-h planning horizon. For the next 23 hours (i.e. t = 1 h to t = 23 h), only SSRO was hourly repeated to update $\mathbf{X_{SSRO}}$ for the planning horizon. $\mathbf{X_{DSRO}}$ was kept as those values determined at t = 0 h in order to ensure that the operating duration of those schedulable electrical appliances would be completed within one day.

4.1.1 Control variables $\mathbf{X_{DSRO}}$ and $\mathbf{X_{SSRO}}$

At the energy demand side, the on/off indicators U_{wm}, U_{dw}, U_{vc}, U_{car1} and U_{car2} of washing machine, dish washer, vacuum cleaner and two electric cars in each flat were chosen as DSRO control variables $\mathbf{X_{DSRO}}$. U = 1 indicated that the corresponding appliance was scheduled to be operating during that hour, while U = 0 was off. As described in Section 2, there are 30 × 6 = 180 flats in the high-rise apartment building. By assuming typical demand patterns in order to save computational time, only 30 flats had different energy demands. Thus the total quantity of each on/off indicator U_{wm}, U_{dw}, U_{vc}, U_{car1} or U_{car2} was 30 only.

At the energy supply side, each category of energy was generated by at least two equipment units. The SSRO control variables were chosen as follows: Operating capacity of SOFC-GT $C_{SOFC\text{-}GT}$, operating capacity of AbC C_{AbC}, operating capacity of CoCs C_{CoC}, recovered thermal energy through HX1 for space heating C_{HX1}, recovered thermal energy through HX2 for bathing water heating C_{HX2}, recovered thermal energy through HX3 for drinking water heating C_{HX3}, recovered thermal energy through HX4 for the AbC C_{HX4}, CS charging rate $r_{ch,c}$, CS discharging rate $r_{dch,c}$, HS charging rate $r_{ch,h}$, HS discharging rate $r_{dch,h}$, ES charging rate $r_{ch,e}$ and ES discharging rate $r_{dch,e}$.

In summary, $\boldsymbol{X}_{DSRO}$ and $\boldsymbol{X}_{SSRO}$ were vectors that composed of 150 (= 5 × 30) and 13 control variables in each hour, respectively: $\boldsymbol{X}_{DSRO}$ = (U_{wm}, U_{dw}, U_{vc}, U_{car1}, U_{car2}), $\boldsymbol{X}_{SSRO}$ = ($C_{SOFC\text{-}GT}$, C_{AbC}, C_{CoC}, C_{HX1},

C_{HX2}, C_{HX3}, C_{HX4}, $r_{ch,c}$, $r_{dch,c}$, $r_{ch,h}$, $r_{dch,h}$, $r_{ch,e}$, $r_{dch,e}$). Namely, $\mathbf{X_{DSRO}}$ and $\mathbf{X_{SSRO}}$ were 150 × 24 and 13 × 24 matrices of control variables, respectively.

4.1.2 Optimization objective function

The objective function was constructed to minimize the daily primary energy consumption (*DPEC*) of the MES. In the developed MES, the primary fuel methane was only consumed by the SOFC-GT set, the objective function was set as:

$$min\ DPEC = \sum_{t=1}^{t=24} [PEC_{SOFC-GT}(t)]\Delta t \quad (1)$$

where $PEC_{SOFC\text{-}GT}$ is the primary energy consumption rate of SOFC-GT ($GJ \cdot h^{-1}$).

4.1.3 Optimization constraints

For DSRO, the total operating duration of each schedulable electrical appliance should meet the requirement shown in the 4th column of Table 4.

$$\sum_{t=1}^{t=24} [U_{wm}(t)] = d_{wm} \quad (2)$$

$$\sum_{t=1}^{t=24} [U_{dw}(t)] = d_{dw} \quad (3)$$

$$\sum_{t=1}^{t=24} [U_{vc}(t)] = d_{vc} \quad (4)$$

$$\sum_{t=1}^{t=24} [U_{car1}(t)] = d_{car1} \quad (5)$$

$$\sum_{t=1}^{t=24} [U_{car2}(t)] = d_{car2} \quad (6)$$

where d_{wm}, d_{dw}, d_{vc}, d_{car1}, d_{car2} were the required operating duration of washing machine, dish washer, vacuum cleaner and two electric cars, respectively.

For SSRO, the optimization constraints included the balance between energy demand and supply, as well as the operating constraints of the associated equipment units. Cooling, heating and electric aspects of energy balance between the supply side (i.e. MES) and the demand side (i.e. high-rise apartment building) are summarized as follows:

$$D_c + r_{ch,c} \leq C_{AbC} + C_{CoC} + r_{dch,c} \quad (7)$$

$$D_h + r_{ch,h} \leq C_{HX1} + C_{HX2} + C_{HX3} + C_{HX4} + r_{dch,h} \quad (8)$$

$$D_e + P_{CoC} + P_{para} + r_{ch,e} \leq C_{SOFC-GT} + r_{dch,e} \quad (9)$$

$$D_e = P_{nsch} + P_{sch} \quad (10)$$

where P_{CoC}, P_{para}, P_{nsch} and P_{sch}, were the electrical power consumption of CoCs, parasitic equipment units in MES, non-schedulable residential electrical appliances, and schedulable electrical appliance, respectively (GJ·h^{-1}). The operating constraints of the associated equipment units were set the same as our previous research [36]: The operating capacity of the SOFC-GT set, AbC, CoCs should not surpass the corresponding maximum and minimum design capacities; energy stored in CS, HS and ES could not outstrip the respective capacities; while energy charge and discharge should not happen simultaneously.

4.2 FC algorithm

In real system operation, the discrepancy of weather forecast would result in deviations between the actual and predicted energy demands. Thus the FC algorithm was involved to revise those pre-determined $\mathbf{X_{SSRO}}$ values within each hour, as shown in Fig. 9. Since it is not practical to adjust the operating capacity of SOFC-GT, AbC and CoC within an hour, only the refined charge/discharge rates of CS, HS and ES (i.e. $r'_{ch,c}$, $r'_{dch,c}$, $r'_{ch,h}$, $r'_{dch,h}$, $r'_{ch,e}$ and $r'_{dch,e}$ respectively) were determined by the FC algorithm in each 15-minute. In other words, there were four control variables $\boldsymbol{X}_{FC,1}$ $\boldsymbol{X}_{FC,2}$ $\boldsymbol{X}_{FC,3}$ $\boldsymbol{X}_{FC,4}$ within each hour, and $\boldsymbol{X}_{FC}$ = ($r'_{ch,c}$, $r'_{dch,c}$, $r'_{ch,h}$, $r'_{dch,h}$, $r'_{ch,e}$, $r'_{dch,e}$). Such algorithm is presented as follows:

if $\Delta D_k > 0$
  if $r_{ch,k} > 0$ **then**
    $r'_{ch,k} = max(r_{ch,k} - \Delta D_k, 0)$
    $r'_{dch,k} = max(\Delta D_k - r_{ch,k}, 0)$
  fi
  if $r_{dch,k} > 0$ **then**
    $r'_{ch,k} = 0$
    $r'_{dch,k} = r_{dch,k} + \Delta D_k$
  fi
fi

if $\Delta D_k < 0$
  if $r_{ch,k} > 0$ **then**
    $r'_{ch,k} = r_{ch,k} - \Delta D_k$
    $r'_{dch,k} = 0$
  fi
  if $r_{dch,k} > 0$ **then**
    $r'_{ch,k} = max(-r_{dch,k} - \Delta D_k, 0)$
    $r'_{dch,k} = max(r_{dch,k} + \Delta D_k, 0)$
  fi
fi

where $k = c, h, e$ for CS, HS and ES, respectively.

4.3 Development of simulation-control platform

To appraise the performance of IDSSM strategy on the complex MES and the high-rise apartment building, the IDSSM method was constructed in MATLAB [39], while the system model of MES, along with the building model, was developed using TRNSYS 17 [40]. To establish the simulation-control platform, the component Type 155 in TRNSYS was employed to link MATLAB with TRNSYS. In DSRO and SSRO of the IDSSM strategy, particle swarm optimization (PSO) was used to find appropriate $\mathbf{X}_{\mathbf{DSRO}}$ and $\mathbf{X}_{\mathbf{SSRO}}$ to minimize the *DPEC*. The parameters used in PSO algorithm is summarized in Table 6, while the detailed interaction and information exchanging between IDSSM in MATLAB and MES in TRNSYS could be found in our previous study [36].

Table 6. Parameters of PSO.

Parameter	**PSO**
Population size	100
Maximum number of iterations	500
Algorithm-specific parameters	Cognitive parameter: 0.5 Social parameter: 3.5 Constriction factor: 0.5

5. Results and discussions

Through the SOFC-GT-primed trigeneration serving the apartment building, the performance appraisal of the IDSSM algorithm was conducted. The effectiveness of DSRO and SSRO was tested first, then the performance of the entire IDSSM method would be assessed.

5.1 Performance evaluation of DSRO and SSRO

To evaluate the performance of DSRO and SSRO, 3 cases were established and compared in order to assess effectiveness of SSRO and DSRO:

Case A: Only SSRO was implemented, and it was assumed that none of the residential electrical appliances could be scheduled.

Case B: Both SSRO and DSRO were implemented, but it was assumed that only the operating duration of electric cars could be scheduled.

Case C: Both SSRO and DSRO were implemented, and the operating duration of all the schedulable electrical appliances would be scheduled.

5.1.1 Analysis of electricity demand distribution and profiles

After implementing RO on each case in four seasons, the resulting daily electrical power consumption is shown in Fig. 10. Here, electricity consumption refers to the total of electrical energy demand of building, CoCs and parasitic equipment units. From Fig. 10, it is seen that the profile of electrical power consumption was similar in Cases B and C, while quite different from Case A:

- For Case A, since DSRO was not implemented, there was a peak electricity consumption during 18^{th} - 20^{th} h in the four seasons, and the peak value would be as high as 12.9 GJ/h in summer.
- For Case B, by applying DSRO on the electric cars, the electricity consumption during 1^{st} – 7^{th} and 19^{th} - 24^{th} was distributed relatively evenly. It was because that the electric cars were not allowed to be charged during 7^{th} -17^{th} h according to Table 4. And the peak consumption was largely reduced to 5.7 GJ/h at the 19^{th} h in summer, which accounted for 44.2% of that in Case A.
- For case C, apart from electric cars, the operating durations of schedulable electrical appliances, including dish washers, washing machines and vacuum cleaners, were also involved. As a result, the peak consumption in Case B was further shifted and distributed in other hours. The value of peak consumption was further decreased to 4.5 GJ/h, which was 34.9% of that in Case A.

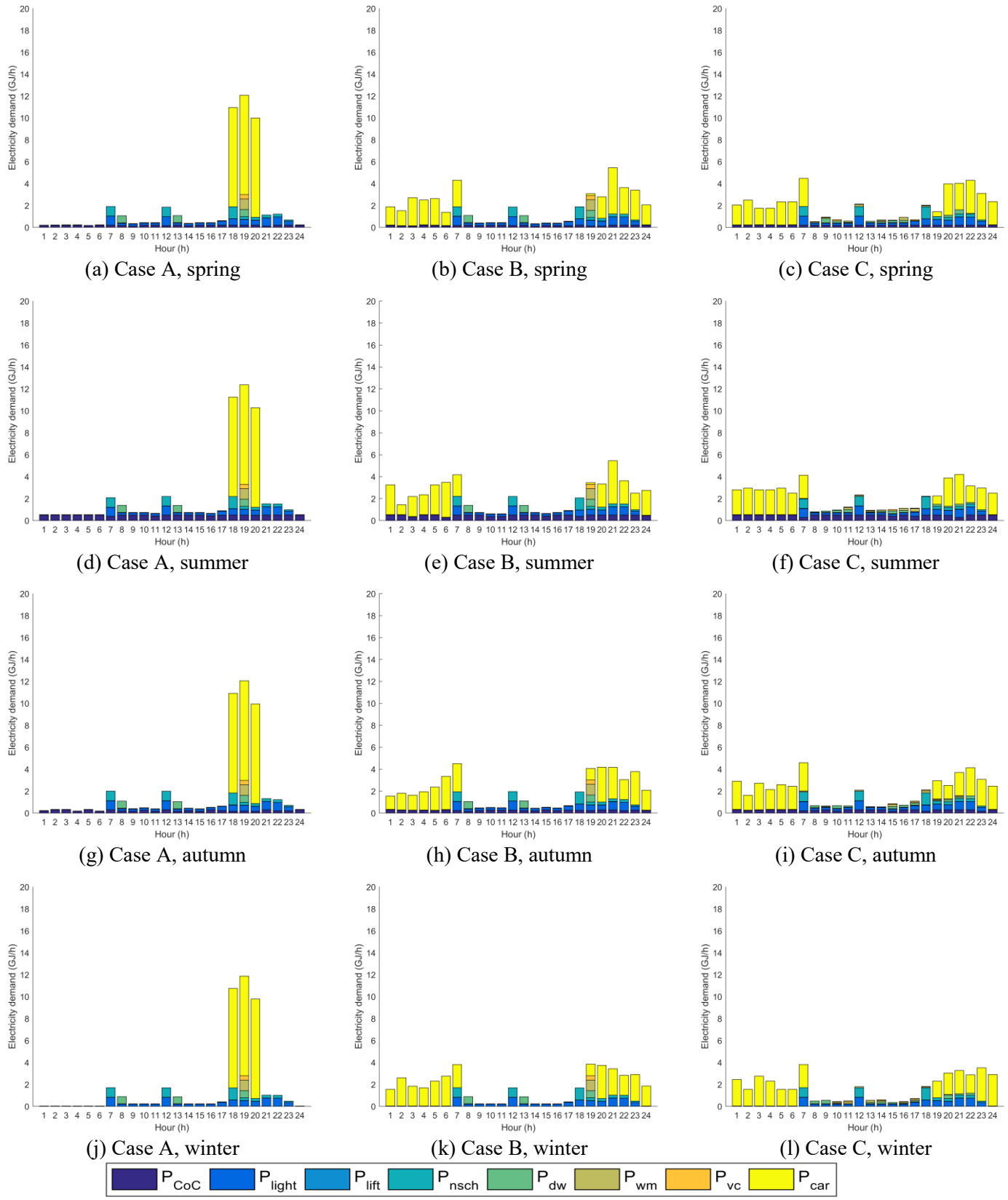

(a) Case A, spring (b) Case B, spring (c) Case C, spring

(d) Case A, summer (e) Case B, summer (f) Case C, summer

(g) Case A, autumn (h) Case B, autumn (i) Case C, autumn

(j) Case A, winter (k) Case B, winter (l) Case C, winter

Fig. 10. Electrical power consumption under RO algorithm on the four representative days.

Overall speaking, by integrating SSRO with DSRO, the peak electricity consumption could be greatly reduced, thus the daily profile became more even. The *DPEC* in each case and each season is summarized in Table 7.

Table 7. Summary of *DPEC*

Case	*DPEC*	Spring	Summer	Autumn	Winter
A	Value (GJ)	144	160	139	131
B	Value (GJ)	138 (↓4.17%)	150 (↓6.25%)	135 (↓2.88%)	129 (↓1.53%)
C	Value (GJ)	133 (↓7.64%)	146 (↓8.75%)	130 (↓6.47%)	127 (↓3.05%)

Through the simultaneous implementation of SSRO and DSRO, besides appropriate operating durations of the electric cars and schedulable electrical appliances could be determined, the operating capacities of energy supply equipment units could also be reduced accordingly. The highest and lowest *DPEC* reduction was 8.75% in summer and 3.05% in winter compared to that when DSRO was not implemented.

5.1.2 Analysis of part-load performances of MES

To better compare the MES performance under different situations, *PLR*s of the SOFC-GT set, AbC and CoCs in different cases and seasons are shown in Fig. 11. PLR_{CoC} would be the same when multiple CoCs operated owing to the reason that identical CoCs were designed.

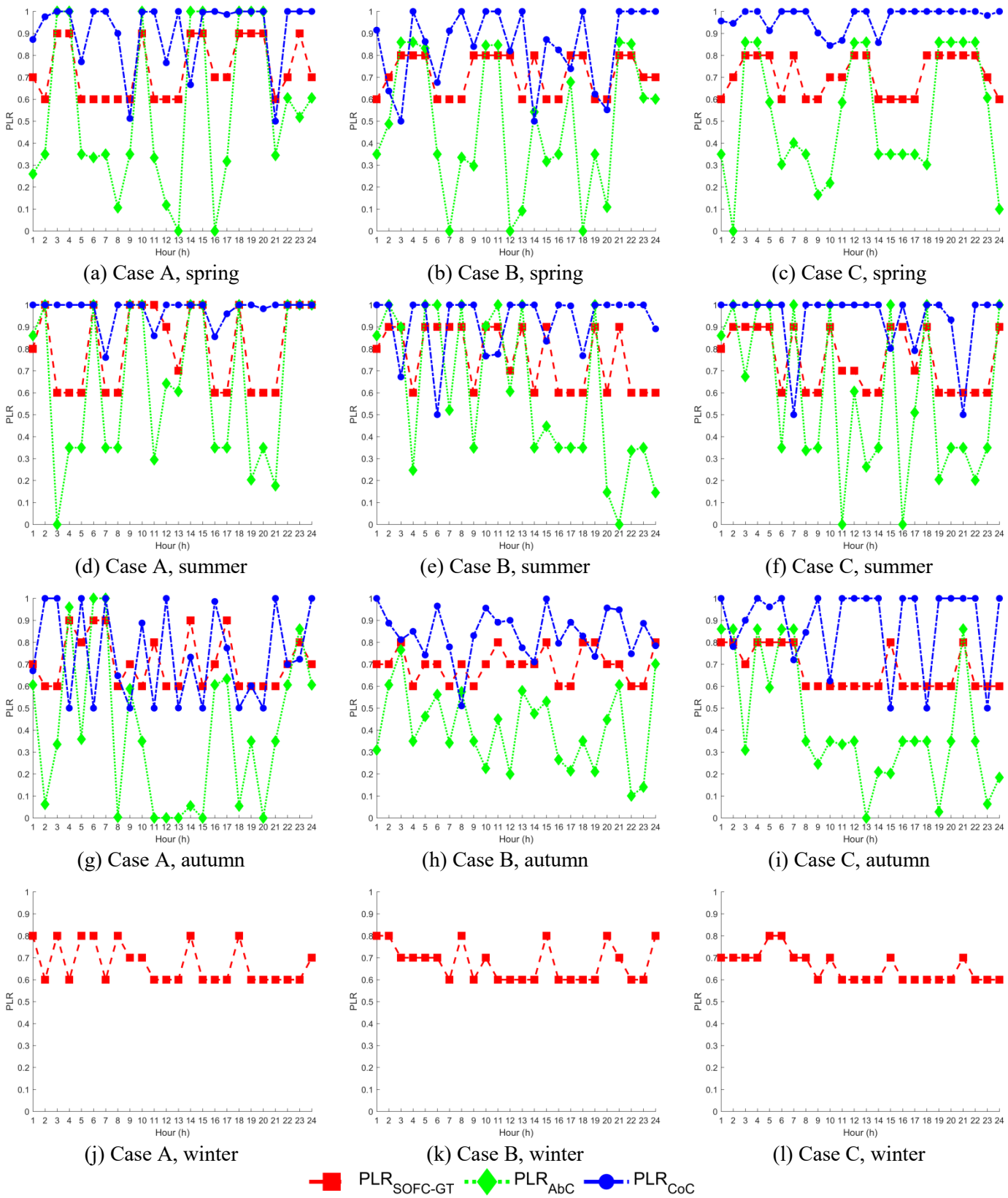

(a) Case A, spring (b) Case B, spring (c) Case C, spring

(d) Case A, summer (e) Case B, summer (f) Case C, summer

(g) Case A, autumn (h) Case B, autumn (i) Case C, autumn

(j) Case A, winter (k) Case B, winter (l) Case C, winter

Fig. 11. *PLR* profiles of RO algorithms on the four representative days.

In Case A, when DSRO was not implemented, the $PLR_{SOFC\text{-}GT}$ was more fluctuated, compared to Cases B and C. For instance, in summer, $PLR_{SOFC\text{-}GT}$ was between 0.6 and 1 in Case A, while only

between 0.6 and 0.9 in Cases B and C. In spring and autumn, $PLR_{SOFC\text{-}GT}$ was between 0.6 and 0.9 in Case A, while between 0.6 and 0.8 in Cases B and C. It was because that the SOFC-GT set had to operate at high $PLR_{SOFC\text{-}GT}$ to satisfy the high electricity consumption in Case A. The frequent variation of $PLR_{SOFC\text{-}GT}$ would also result in higher primary energy consumption due to the heat-up process of the SOFC stack. The SOFC-GT set were not in full-load operation in Cases B and C, since the design capacity was determined according to the situation in Case A. In fact, the design capacity of the SOFC-GT set could be smaller in Cases B and C, which would also result in more full-load operation and lower capital cost.

For AbCs, PLR_{AbC} depended on various scenarios. For example, the exhaust heat from the SOFC-GT set was recovered for both apartment heating demand and AbC operation; the recovered thermal energy could be stored in HS; and the produced chilled water could be stored in CS. Therefore, PLR_{AbC} could be quite fluctuated and did not follow a certain pattern. For CoCs, the operating quantity was set different in 3 seasons in order to let them operate at full-load as far as possible. Meanwhile, the SSRO would also find the opportunity to operate CoCs at part-load to reduce their electrical power consumption. As a result, PLR_{CoC} also varied with seasons of different cases, but it was not as fluctuating as PLR_{AbC}.

Consequently, it was found that simultaneous implementation of SSRO and DSRO algorithms could help coordinate the MES operation and building electricity demand in different seasons. Moreover, city power grid was only connected for emergency purpose, indicating that the design of the MES was self-sufficient in different situations of energy supply.

5.1.3 Analysis of different energy contributions of MES

To further test the performance of SSRO and DSRO algorithms, operating capacity allocation in the corresponding cooling, heating and electrical energy supply equipment units were studied. Values of energy stored in CS, HS and ES were also involved and represented by e_{CS}, e_{HS} and e_{ES} respectively.

Fig. 12 illustrates the cooling energy profiles in different seasons of the 3 cases. It is seen that AbC, CoCs and CS could collaborate to satisfy the predicted cooling demand at any time in each day. Since it was only appropriate to slightly schedule the cooling demand due to the thermal comfort requirement, the profiles of cooling demand were similar among three cases. It was found that the cooling demand had a peak during the 21st - 22nd h, and it was relatively low during daytime.

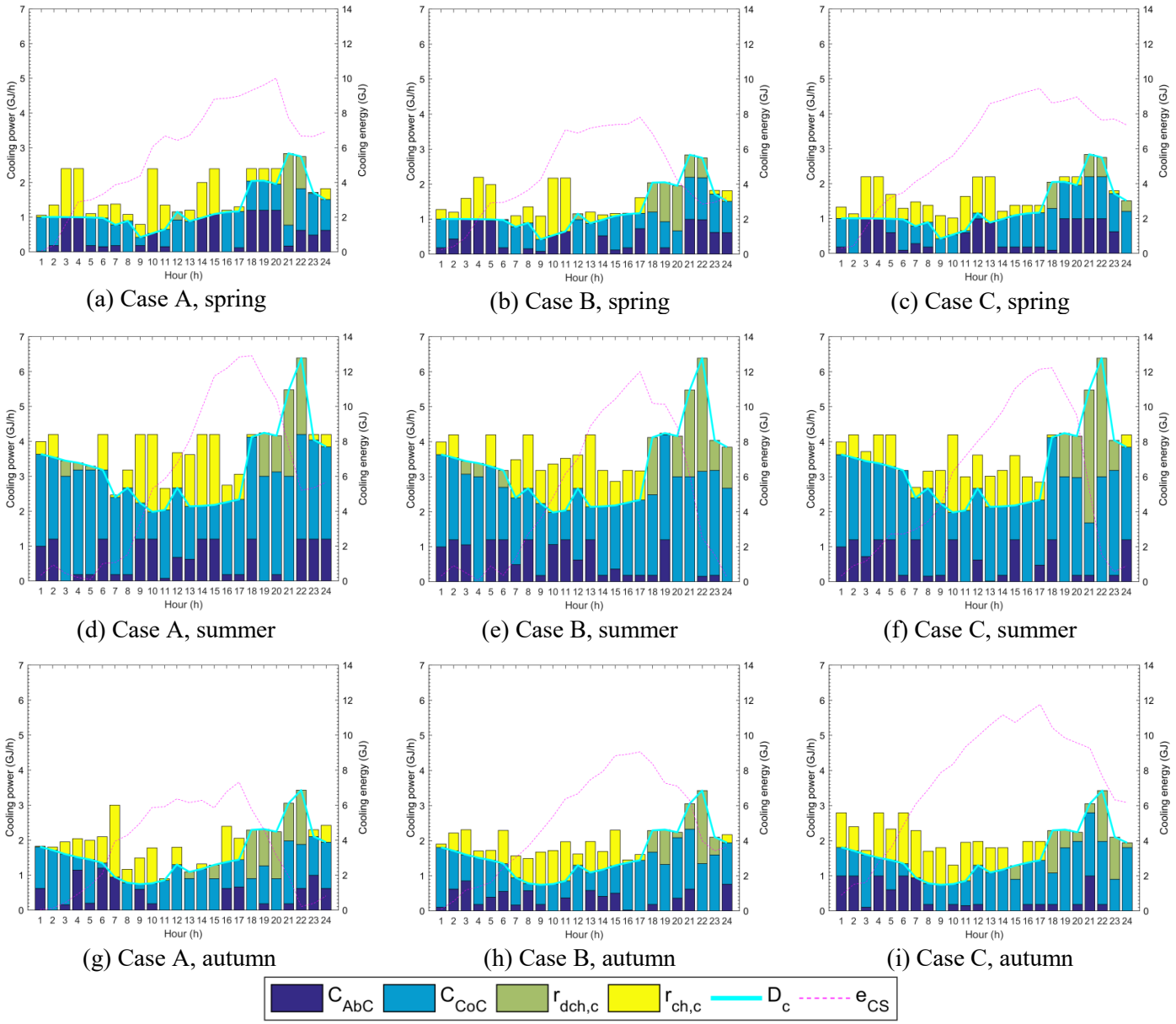

(a) Case A, spring (b) Case B, spring (c) Case C, spring

(d) Case A, summer (e) Case B, summer (f) Case C, summer

(g) Case A, autumn (h) Case B, autumn (i) Case C, autumn

Fig. 12. Cooling energy supply allocation under DSRO and SSRO algorithm on the four representative days.

For all cases, AbC was firstly scheduled to operate, followed by CoCs. CS would also be discharged to supplement cooling demand when necessary, especially at the night time. For the high-rise apartment building, CS was charged during most of the time during the 1st-17th h. After the 17th h, CS would be discharged to provide enough cooling supply during the high cooling demand.

Fig. 13 depicts the profiles of $D_{h,t}$, the total heating demand of the apartment building and the thermal energy required by AbC, in various seasons of the three cases. The recoverable thermal energy from the SOFC-GT set was decided by its operating capacity . Thus, the peak $D_{h,t}$ in Cases B or C could be lower than that in Case A.

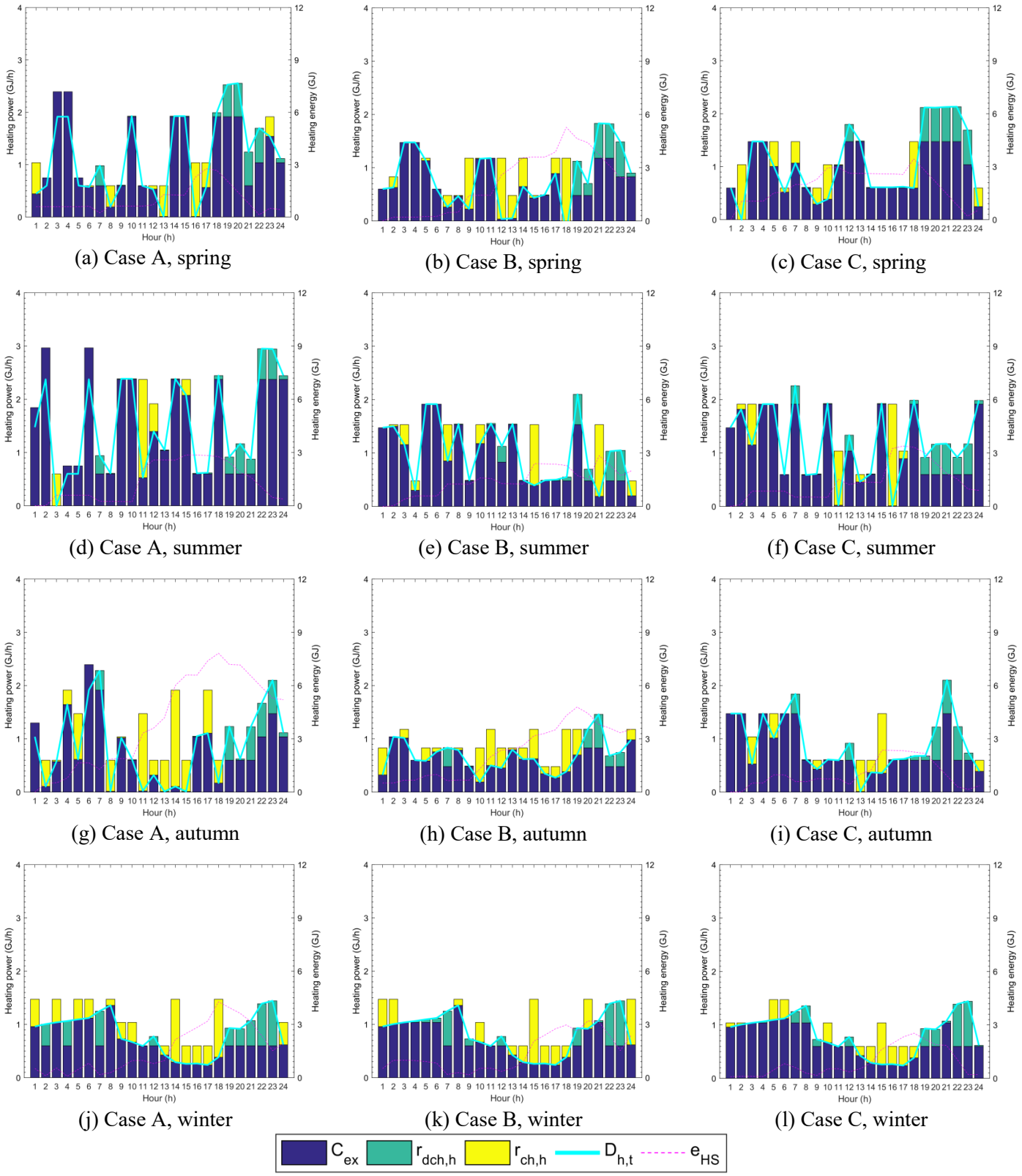

(a) Case A, spring (b) Case B, spring (c) Case C, spring

(d) Case A, summer (e) Case B, summer (f) Case C, summer

(g) Case A, autumn (h) Case B, autumn (i) Case C, autumn

(j) Case A, winter (k) Case B, winter (l) Case C, winter

Fig. 13. Heating energy supply allocation under DSRO and SSRO algorithm on the four representative days.

Fig. 14 shows the profiles of electrical power contribution in different cases. In each case, SOFC-GT set and ES could properly work together to satisfy the electrical energy demand on the four representative days. For Case A, large amount of electrical energy was discharged from ES during the 18^{th} – 20^{th} h. The ES was charged during all the other time period. For Cases B and C, ES was discharged during 7^{th} and 19^{th}-24^{th} h in most of the seasons since the electricity consumption was relatively high during those hours. However, the discharging rate was much reduced due to lower electricity consumption compared to that in Case A. Moreover, the maximum energy stored in ES in Case C was 20 GJ, which was 43% lower than that in Case A (35 GJ). Therefore, through the integrating DSRO with SSRO, the design capacity, thus the capital cost and spatial requirement of ES could be largely decreased. Moreover, the charging and discharging processes of ES would cause additional energy loss, thus the lower $r_{ch,e}$ and $r_{dch,e}$ would help acquire the minimum *DPEC*.

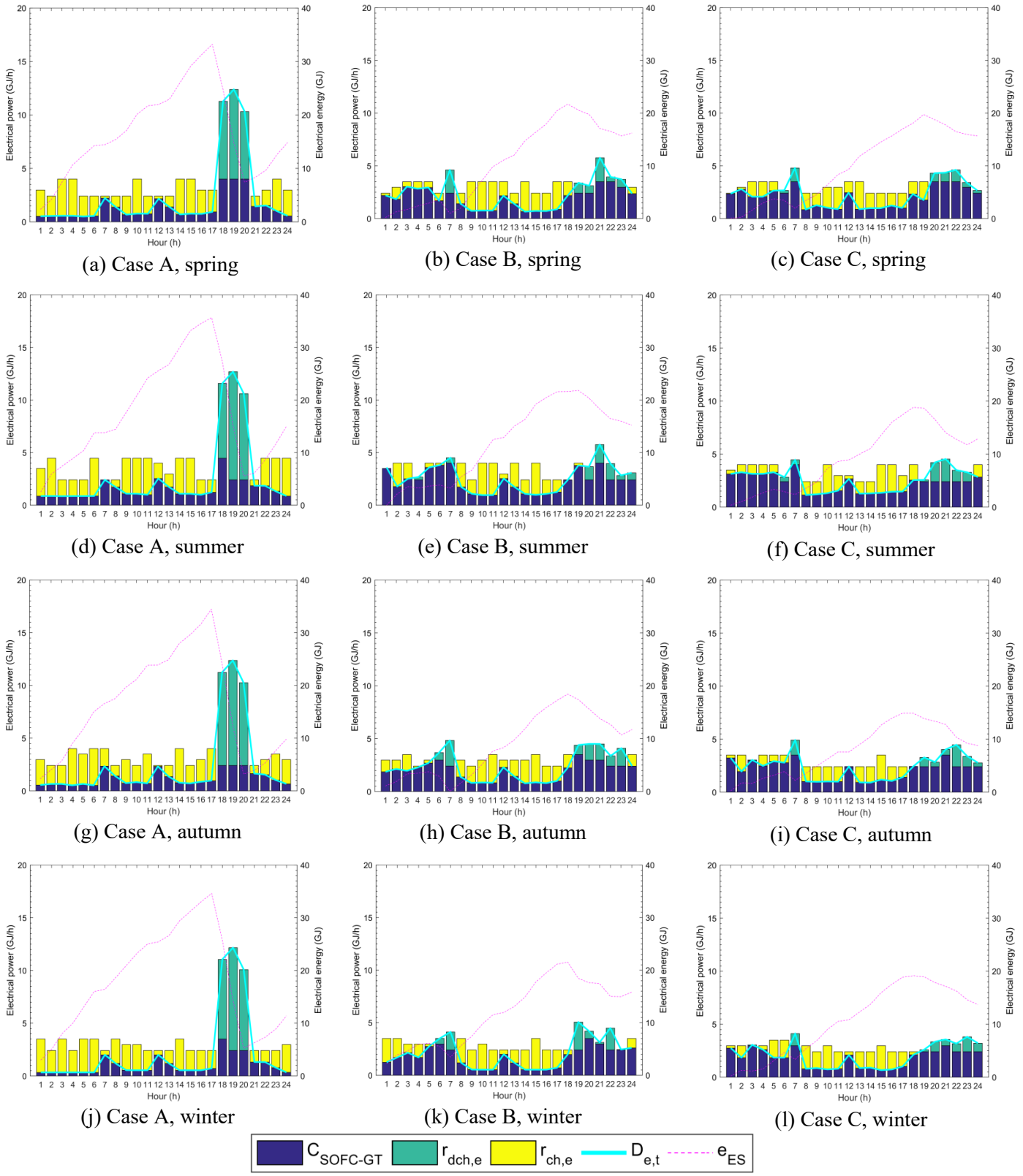

(a) Case A, spring (b) Case B, spring (c) Case C, spring

(d) Case A, summer (e) Case B, summer (f) Case C, summer

(g) Case A, autumn (h) Case B, autumn (i) Case C, autumn

(j) Case A, winter (k) Case B, winter (l) Case C, winter

Fig. 14. Electrical energy supply contribution under RO algorithm on the four representative days.

5.2 Performance evaluation of entire IDSSM strategy

After ensuring the effectiveness of integrated DSRO and SSRO, the whole IDSSM strategy was adopted to investigate how the energy supplies from the MES could match with the actual demands of the high-rise apartment building in each 15-minute throughout a day. Based on Case C, the operating capacity contributions from the corresponding equipment units for different supplies are shown in Fig. 15.

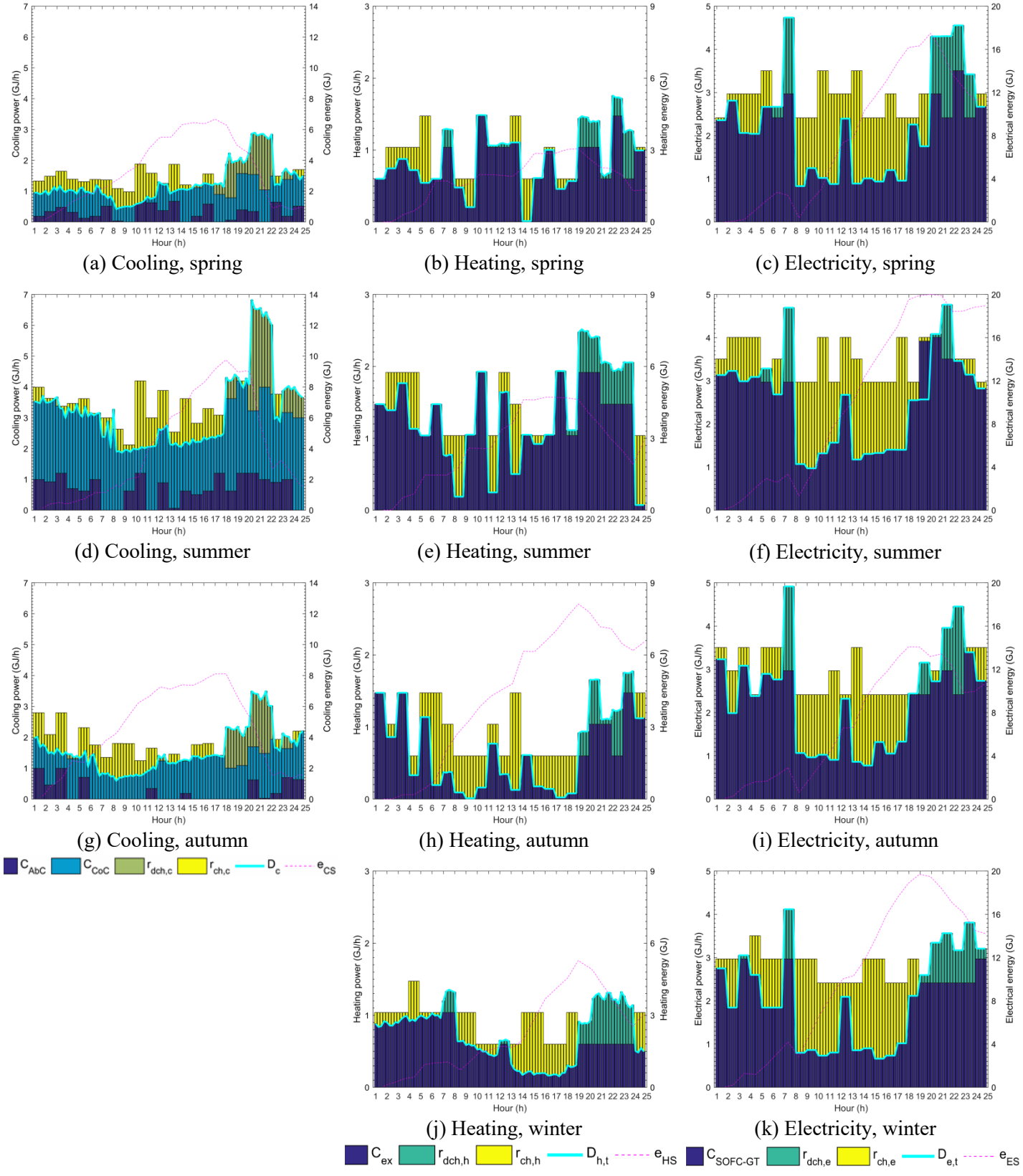

Fig. 15. Cooling, heating and electrical energy supply allocation under IDSSM strategy on the four representative days.

From Fig. 15, it is observed that the energy supplies and demands of cooling, heating and electricity can be well in line with each other. This is because the FC algorithm could determine the revised

charging/discharging rates of the related energy storages, thus make efficient corrections according to the prediction errors of energy demands. Thus the cooling, heating and electrical energy provided by the MES could sufficiently satisfy the corresponding demands.

5. Conclusion

This paper proposed the IDSSM strategy for handling the complex MES and multiple building energy demands, which could be independent on the availability of incentive electricity schemes. To demonstrate effectiveness of the proposed control strategy, a SOFC-GT primed trigeneration with three types of energy storages was adopted as MES, serving a high-rise apartment building featured with electric cars and other schedulable electrical appliances. The IDSSM method included three core algorithms: DSRO, SSRO and FC. In the first hour on each day, operating durations of the schedulable electric appliances were determined by DSRO. Meanwhile, operating schedule of the energy supply equipment units in MES was decided by SSRO. During the next 23 hours, SSRO was repeated to update the schedule of the operating variables for MES. Within the implementation interval of SSRO, FC was applied for continual mitigation whenever there existed any difference between the actual and predicted energy demands in each 15-minute.

In this study, the dynamic simulation model of the holistic MES and the apartment building was built in TRNSYS, with the part-load performances of SOFC-GT set, AbC and CoCs taken into account. The IDSSM algorithm was written in MATLAB and connected with TRNSYS to simulate the actual control implementation. The proposed IDSSM strategy was found to have the following distinctive merits:

- When SSRO was integrated with DSRO, the peak electrical power consumption was 44% compared to the scenario without DSRO. In this regard, 8.75% primary energy consumption could be decreased. Meanwhile, the design capacities of ES and SOFC-GT set could be reduced to 57% and 90% of the original capacities respectively. Electric cars could make a significant contribution to the DSRO due to their relatively large electrical power consumption.
- Through minimizing *DPEC*, effective demand and load shifting could be obtained through close coordination among electric cars, other schedulable electrical appliances and energy supply equipment units. The daily profiles of cooling, heating and electrical energy demands could be considered by the SSRO and DSRO algorithms.
- FC algorithm could effectively rectify the inconsistencies between the actual and predicted energy demands. As a result, different energy supplies provided by the MES could be well matched with the corresponding building demands, avoiding unnecessary surplus or deficit.

In conclusion, the IDSSM strategy could provide an integrative approach of demand and supply side energy management. In the demand side, the peak electrical power consumption would be shifted in those required periods. In the supply side, appropriate *PLR*s of the SOFC-GT set, AbC and CoC could be searched to minimize *DPEC* of the MES. The proposed IDSSM strategy can be further extended to wider application, like micro-grid for a residential community.

Acknowledgement

This work described in this paper is fully supported by a grant from the Research Grants Council of the Hong Kong Special Administrative Region, China (Project No. CityU 11200315).

Nomenclature

C	Capacity ($GJ \cdot h^{-1}$)
COP	Coefficient of performance
D	Energy demand ($GJ \cdot h^{-1}$)
$DPEC$	Daily primary energy consumption ($GJ \cdot day^{-1}$)
d	Duration (h)
e	Stored energy (GJ)
P	Electrical power ($GJ \cdot h^{-1}$)
PEC	Primary energy consumption rate ($GJ \cdot h^{-1}$)
PLR	Part-load ratio
r	Charging/discharging rate ($GJ \cdot h^{-1}$)
RH	Relative humidity (%)
T	Temperature (°C)
U	On/off state (0 or 1)
$\boldsymbol{X}_{FC}$	Vector of control variables of FC
$\boldsymbol{X}_{DSRO}$	Vector of control variables of DSRO
$\boldsymbol{X}_{SSRO}$	Vector of control variables of SSRO
$\mathbf{X}_{\mathbf{DSRO}}$	Matrix of control variables of DSRO
$\mathbf{X}_{\mathbf{SSRO}}$	Matrix of control variables of SSRO

Greek symbols

Δ	Difference between the actual and predicted values
Δt	Time interval (h)

Subscripts

AbC	Absorption chiller
b	Basic
c	Cooling energy
car1, car2	Electric car
ch	Charge
CoC	Compression chiller
db	Dry-bulb
dch	Discharge
dw	Dish washer
e	Electrical energy
f	Forecasted
h	Heating energy
k	Type of energy (i.e. cooling, heating and electrical energy)
ns	Non-schedulable electrical appliances
p	Predicted
para	Parasitic equipment
r	Actual
REC	Recovered
sch	Schedulable electrical appliances
SP	Space heating
vc	Vacuum cleaner
WH	Water heating
wm	Washing machine

Abbreviations

AbC	Absorption chiller
CoC	Compression chiller
CS	Cool storage
DSM	Demand side management
DSRO	Demand side rolling optimization
ES	Electricity storage
FC	Feedback correction
GT	Gas turbine
HS	Heat storage
HX	Heat exchanger

IDSSM	Integrated demand and supply side management
MES	Multi-energy system
PSO	Particle swarm optimization
SOFC	Solid oxide fuel cell
SSM	Supply side management
SSRO	Supply side rolling optimization

References

[1] Transition to Sustainable Buildings. Executive summary. IEA 2013.

[2] Mancarella Pierluigi. MES (multi-energy systems): an overview of concepts and evaluation models. Energy. 65(2014)1–17.

[3] Wu DW and Wang RZ. Combined cooling, heating and power: a review. Progress in Energy and Combustion Science. 32(2006)459-95.

[4] Wang CS, Jiao BQ, Guo L, Tian Z, Niu JD and iwei Li. Robust scheduling of building energy system under uncertainty. Applied energy. 167(2016)366-376.

[5] Sanjari MJ, Karami H and Gooi HB. Micro-generation dispatch in a smart residential multi-carrier energy system considering demand forecast error. Energy Conversion and Management. 120(2016)90-99.

[6] Bischi A. A detailed MILP optimization model for combined cooling, heat and power system operation planning. Energy. 74(2014)12-26.

[7] Wakui T, Ryohei Y and Shimizu K. Suitable operational strategy for power interchange operation using multiple residential SOFC (solid oxide fuel cell) cogeneration systems. Energy. 35(2010)740-750.

[8] Kriett PO and Salani M. Optimal control of a residential microgrid. Energy. 42(2012)321-330.

[9] Wu Q, Ren HB, Gao WJ and Ren JX. Multi-objective optimization of a distributed energy network integrated with heating interchange. Energy. 109(2016)353-364.

[10] Monyei CG and Adewumi AO. Integration of demand side and supply side energy management resources for optimal scheduling of demand response loads–South Africa in focus. Electric Power Systems Research. 158(2018)92-104.

[11] Batić M, Nikola T, Giovanni B, Turhan D and Sanja V. Combined energy hub optimisation and demand side management for buildings. Energy and Buildings. 127(2016)229-241.

[12] Farsangi, Alireza S, Shahrzad H, Mehdi M and Heidarali S. A novel stochastic energy management of a microgrid with various types of distributed energy resources in presence of demand response programs. Energy. 160(2018)257-274.

[13] Okae J, Juan Du, Akowuah EK, Appiah G and Anto EK. The Design and Realization of Smart Energy Management System based on Supply-Demand Coordination. IFAC-Papers OnLine. 50(2017)195-200.

[14] Silvente J, Kopanos GM, Efstratios NP and Antonio E. A rolling horizon optimization framework for the simultaneous energy supply and demand planning in microgrids. Applied Energy. 155(2015)485-501.

[15] Silvente J, Aguirre MA, Zamarripa MA, Méndez CA, Moisès G and Antonio E. Improved time representation model for the simultaneous energy supply and demand management in microgrids. Energy. 87(2015)615-627.

[16] Kienzle F, Peter A and Göran A. Valuing investments in multi-energy conversion, storage, and demand-side management systems under uncertainty. IEEE Transactions on Sustainable Energy. 2(2011)194-202.

[17] Ahčin P and Mario Š. Simulating demand response and energy storage in energy distribution systems. In Power System Technology (POWERCON). 2010 International Conference. IEEE. (2010)1-7.

[18] Henning Dag. Cost minimization for a local utility through CHP, heat storage and load management. International Journal of Energy Research. 22(1998)691-713.

[19] Brahman F, Masoud H and Shahram J. Optimal electrical and thermal energy management of a residential energy hub: integrating demand response and energy storage system. Energy and Buildings. 90(2015)65-75.

[20] Ma TF, Wu JY and Hao LL. Energy flow modeling and optimal operation analysis of the micro energy grid based on energy hub. Energy Conversion and Management. 133(2017)292-306.

[21] Zhang Y, Zhang T, Wang R, Liu Y and Guo B. Optimal operation of a smart residential microgrid based on model predictive control by considering uncertainties and storage impacts. Solar Energy. 122(2015)1052-1065.

[22] Mbungu NT, Bansal RC, Naidoo R, Miranda V and Bipath M. An optimal energy management system for a commercial building with renewable energy generation under real-time electricity prices. Sustainable Cities and Society. 41(2018)392-404.

[23] Jin C, Tang J and Ghosh P. Optimizing electric vehicle charging with energy storage in the electricity market. IEEE Trans. Smart Grid. 4(2013)311-320.

[24] Brahman F, Honarmand M and Jadid S. Optimal electrical and thermal energy management of a residential energy hub, integrating demand response and energy storage system. Energy and Buildings. 90(2015)65-75.

[25] Honarmand M, Zakariazadeh A and Jadid S. Integrated scheduling of renewable generation and electric vehicles parking lot in a smart microgrid. Energy Conversion and Management. 86(2014)745-755.

[26] Honarmand M, Zakariazadeh A and JadidS. Self-scheduling of electric vehicles in an intelligent parking lot using stochastic optimization. Journal of the Franklin Institute. 352(2015)449-467.

[27] Bojic M, Yik F, Sat P. Influence of thermal insulation position in building envelope on the space cooling of high-rise residential buildings in Hong Kong. Energy and Buildings. 33(2001)569-81.

[28] Bojic M, Yik F, Sat P. Energy performance of windows in high-rise residential buildings in Hong Kong. Energy and Buildings. 34(2002)71-82.

[29] Bojic M, Yik F, Wan K, Burnett J. Influence of envelope and partition characteristics on the space cooling of high-rise residential buildings in Hong Kong. Building and Environment. 37(2002)347-55.

[30] Cheung CK, Fuller RJ and Luther MB. Energy-efficient envelope design for high-rise apartments. Energy and Buildings. 37(2005)37-48.

[31] Guidelines on Performance-based Building Energy Code. Electrical & Mechanical Services Department, the Hong Kong Special Administrative Region. 2007.

[32] Code of Practice for Energy Efficiency of Building Services Installation. Electrical & Mechanical Services Department, the Hong Kong Special Administrative Region. 2012.

[33] Chan ALS, Chow TT, Fong SKF, Lin JZ. Generation of a typical meteorological year for Hong Kong. Energy Conversion and Management 47 (2006) 87-96.

[34] AccuWeather. Website: http://www.accuweather.com/en/hk/hong-kong/1123655/hourly-weather-forecast/1123655 (last accessed on 1 November 2018).

[35] Macdonald IA. Quantifying the effects of uncertainty in building simulation. Diss. University of Strathclyde, 2002.

[36] Luo XJ and Fong KF. Development of multi-supply-multi-demand control strategy for combined cooling, heating and power system primed with solid oxide fuel cell-gas turbine. Energy Conversion and Management. 154(2017)538-561.

[37] Luo XJ and Fong KF. Development of 2D dynamic model for hydrogen-fed and methane-fed solid oxide fuel cells. Journal of Power Sources. 328(2016)91-104.

[38] Luo XJ. Development of Dynamic Model and Control Strategy of Combined Cooling, Heating and Power System Primed with Solid Oxide Fuel Cell-Gas Turbine for Building Application. PhD Thesis. City University of Hong Kong. 2018.

[39] MATLAB and Statistics Toolbox Release 2012b, The MathWorks, Inc., Natick, Massachusetts, United States.

[40] TRNSYS 17: A Transient System Simulation Program. Solar Energy Laboratory University of Wisconsin, Madison, USA.